THE LUMINESCENT CHAMBER AND OTHER NEW DETECTORS

L. W. Jones (*) **and M. L. Perl**

University of Michigan, Ann Arbor, Mich.

(presented by L. W. Jones)

I. INTRODUCTION

It is now possible to record photographically single photons of optical wavelength using image intensifier vacuum tubes. This makes possible the luminescent (or scintillation) chamber wherein tracks of ionizing particles in scintillators are recorded with a spatial resolution approaching that of graphical detectors and a time resolution characteristic of particle counters. With the additional flexibility made possible by post-event triggering, this new detector shows promise of wide use in high-energy particle physics [1].

II. REQUIREMENTS

Basically, a luminescent chamber system consists of a scintillator (either a homogeneous solid or a volume filled with light-piping fibers), an image-intensifying electron-optical system, and an image-recording film or television system. Since the information available is limited by the small number of photons available at the source (the path of the particle through the scintillator), it is important to use scintillators of high scintillation efficiency and to use image tube systems capable of recording an appreciable fraction ($>10\%$) of the photons from the scintillator incident on the cathode of the first tube.

Table I lists the relevant characteristics of the scintillators of greatest interest. The values given for cesium iodide, unactivated and cooled to liquid nitrogen temperatures, make it appear a very attractive material; however, measurements in the authors' laboratory have not confirmed the very high efficiency reported in the literature [2]. Very possibly, trace impurities may cause great variations from sample to sample, depending on the supplier and method of crystallization. The crystals [2] were crystallized from aqueous solution, while the sample we measured was crystallized from the melt. Our measurements did

TABLE I

Properties of scintillators

Material	(dE/dx) (**)	Efficiency	Density	N light (**) quanta per cm of track (approximately)
Plastic scintillator	2.0 MeV g/cm^{-2}	~2%	1.05	10^4
NaI : Tl	1.3	8%	3.67	10^5
CsI (77°K) (***)	1.2	50%	4.5	10^6

(*) Currently at the Lawrence Radiation Laboratory, Berkeley, California.

(**) For minimum ionization.

(***) Hahn and Rossel; Knœpfel, Lœpfe, and Stoll.

show a striking pulse height increase from CsI as the temperature was lowered, however at 77° K the pulse height was comparable to that from room temperature, NaI:Tl. This is in agreement with results from other laboratories.

Commercially available " fast " film such as Kodak Royal-X Pan requires about 2×10^8 photons (near 4400 Å) per square centimeter of emulsion for a visually detectable developed density increase (0.1 to 0.2). If the image of a single photon occupies 10^{-3} or 10^{-4} square centimeters on the film, and if the efficiency of the photocathode is 20%, an image intensification of at least 10^4 must be provided. In practice, a gain of 10^5 seems a minimum for good images although improved resolution would lower this requirement. Due to the long component of the light output of efficient phosphors, the gain of image tubes as used in short pulsed applications is generally less than the steady-state gain of the same system.

III. IMAGE TUBE SYSTEMS

Unlike other " chambers " such as the bubble chamber and cloud chamber, the luminescent " chamber " is a passive, static block of material with negligible support and containment problems. However, the " camera ", in this case the image tube system, is the complex part of the system. Figure 1 illustrates a typical single-stage image tube. The image tube gain G should be given by

$$G = \frac{e\varepsilon V}{hv}$$

where e is the cathode efficiency, ε is the anode efficiency, V is the electron accelerating voltage, and hv is the energy of the quanta in electron volts. Gains of 30 to 100 are typical for tubes operated at 10 000 to 30 000 V.

To achieve a gain of 10^5, several tubes must be combined. Zavojskij [1] used several stages of magnetically-focused image tubes in one vacuum envelope, with the phosphor of one section and the photocathode of the following section deposited on opposite sides of a thin transparent film to preserve resolution. Such a tube achieved the required gain; however, its usefulness may be limited due to the small cathode diamteter (0.5 cm) (Fig. 2).

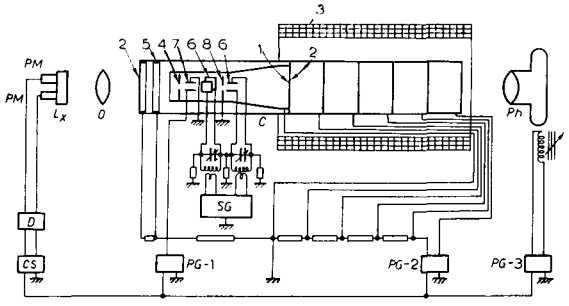

Fig. 2 Zavojskij five-stage magnetically-focused image tube.

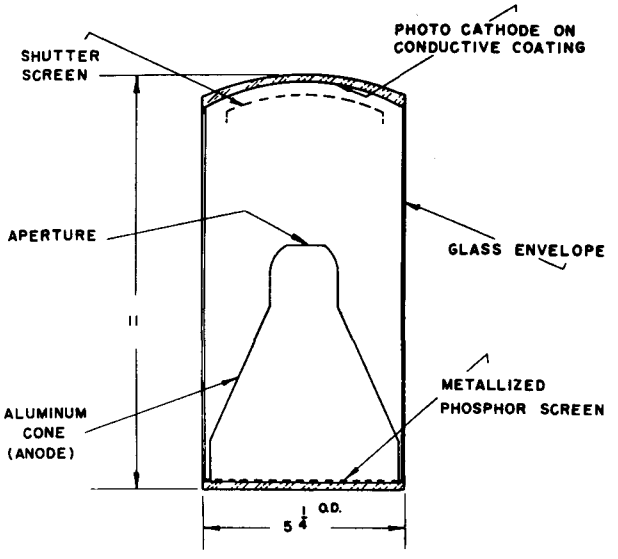

Fig. 1 Single stage electrostatically-focused image tube (from Du Mont Laboratories).

The groups working in the United States [1] have used one and two-stage tubes in a cascade geometry coupled by refractive optics. The two most readily available tubes in the United States are a 12.5 cm cathode, 2.5 cm anode one-stage tube (typical gain at 30 keV of 100) manufactured by the Westinghouse Electric Corporation and a 2.5 cm cathode, 2.5 cm anode two-stage tube (total gain at 10 kV per stage of 300 to 2000) manufactured by the Radio Corporation of America. These are both electrostatically-focused tubes. Unfortunately, the electron optics of the two-stage tube represents some compromise so that the distortion and edge-resolution limit its usefulness; frequently in practice only the central 1.5 cm cathode area is used. The center resolution of these tubes is 12 to 15 line pairs per millimeter. A typical arrangement of image tubes is illustrated in Figure 3. Here, three two-stage tubes are coupled

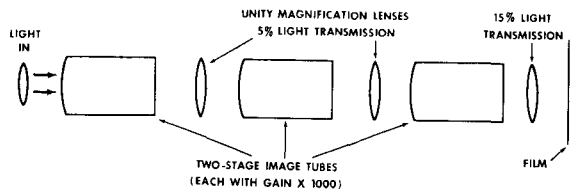

Fig. 3 Cascaded image tube geometry using three two-stage tubes.

by refractive lenses with another refractive lens coupling the last tube to the photographic film. Each tube may have a gain of 1000; each of the two coupling lenses transmits 5% of the light from the preceeding tube; the last lens may transmit 15% of the light from the last tube to the film. Thus the overall gain of this system is given by

$$10^3 \times 5 \times 10^{-2} \times 10^3 \times 5 \times 10^{-2} \times 10^3 \times 15 \times 10^{-1} = 3.8 \times 10^5.$$

This would be the steady-state gain. As used, with gate widths of one to ten milliseconds, the gain is reduced approximately by a factor of four since these tubes are provided with phosphor type P11 or P20. The characteristics of these phosphors may be very roughly represented by a 150 μs time constant and a 10 ms time constant, each accounting for about half of the light.

Gating of the image tubes is necessary not only to provide time resolution for the luminescent chamber, but to avoid fogging the film by the continuous background of the tubes. The simplest method of gating the tubes is to bias the image tube cathode positive with respect to the first focusing electrode to cut-off and then to ground it electronically (to its normal operating voltage) during the gate-on period. For gate lengths less than one microsecond, the cathode resistivity may limit this method, in which case it may be more desirable to bias the focusing electrode negative and pulse it positive to its normal operating voltage. The entire tube voltage may also be pulsed without much difficulty, however, requiring pulse voltages an order of magnitude greater than the above methods. With the system illustrated in Figure 3 and photographed in Figure 4, gate lengths of 0.5 to 2 ms are applied to the second tube, and of 10 ms to the third tube (the first tube is left on continuously), in poor time resolution experiments with cosmic ray tracks.

The image tube background from the two-stage tubes varies between 10^8 and 10^{10} quanta per second from the anode for good tubes. This corresponds to an equivalent input of 10^5 to 10^8 quanta per second. The background from the large cathode one-stage tube is typically 1 to 3×10^9 quanta per second or an equivalent input of about 3×10^7 quanta per second. On both tubes the background seems to increase exponentially with voltage, so that each tube is operated at a voltage where its gain is as high as possible without excessive background. The background seems to be from two sources, positive ion bombardment and cold emission. Tubes known to have a poor vacuum exhibit scintillations clustered axially, presumably due to the axial focusing of positive ions formed in the residual gas by photo-electrons and accelerated across the tube. The scintillations may be shown to result from 10 to 100 electrons from a point on the cathode rather than single electrons. The other source of noise, present even in tubes with very good vacuum, consists of several scintillations per second uniformly distributed over the anode. These may be due to surface phenomena on the photocathode, although again they arise from more than 10 electrons per scintillation. Background due to single electrons from the cathode seems to be much less important than the above.

The image tube phosphors are approximately Lambertian surfaces, therefore the fraction of the light collected by a lens subtending a cone of half angle θ from the anode is approximately given by $\sin^2\theta$. Large aperture lenses measured by the authors transmit 50% to 80% of the light they subtend. As the RCA image tubes have convex photocathodes, either special curved-field lenses must be used or field flatteners (a double concave lens cemented to the cathode) provided to approximately correct for ordinary lenses. A curved-field lens is being developed for this purpose which will transmit 10% of the light, and field flatteners are commonly used with lenses transmitting 5% of the light. Larger aperture lenses may be more readily used for coupling the flat output phosphor to the film.

A promising alternative to the coupling lenses is the fiber optics system[3]. Here the cathode and anode face plates of the image tubes would be made of vacuum tight bundles of glass fibers bonded by a glass frit of lower index of refraction. Light is

" piped " in an image-preserving way without loss of resolution (beyond the fiber diameter) with high efficiency. Such fiber windows of successive stages could then be butted together in a simple way. Glass fiber windows are currently available and are being incorporated into some image tubes. Current fiber diameters in such windows are about 0.08 mm, which corresponds to a resolution almost comparable to the image tube.

It should be noted that in a cascaded system the resolution deteriorates as the resolutions of the components combined in quadrature. Thus three tubes and three lenses, each component with a resolution of 15 line pairs per mm, would have a resultant resolution of $15/\sqrt{6}$ or about 6 line pairs per mm. With currently available tubes and lenses, the resolution obtained on the film corresponds to only 50 to 100 resolved image elements across a 1.5 cm diameter area.

Image tubes may be used with electron-optical regeneration to achieve very high gains. Typical systems are illustrated in Figure 5, where mirror optics focus light from a phosphor back to the cathode of the same image tube. If the image tube has reasonable freedom from distortion (1 % or less), regeneration may be achieved by gating on the image tube for a short time interval. The resulting image will be composed of the superposed images from successive regeneration cycles. The number of times the image must circulate is greater than the number of stages of image tube necessary in a cascade system, so that the resolution will deteriorate more noticeably. If successive images are " out of registry ", a point will be imaged to a series of dots. For a finite gate time, the authors have shown analytically [4] that the brightnesses of successive images near the brightest are nearly equal, so that such an image would be difficult to use. This problem may be circumvented by using two image tubes, or one two-stage tube, and alternatively turning one on and the other off. The brightness ratio between successive images may be an order of magnitude in this flip-flop system, and the number of times the image must traverse an image tube is less than in simple regeneration, although still more than in the cascaded system. An analysis of such " flip-flop " regeneration may be found in papers by the authors [4].

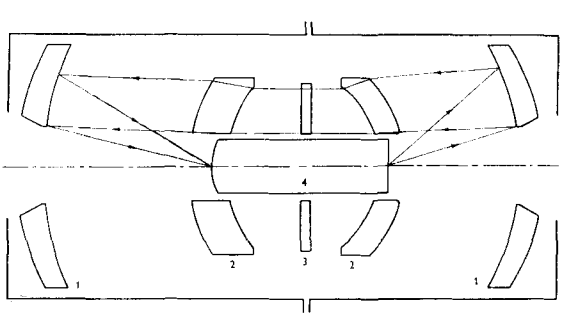

Fig. 5 Regeneration system employing reflective optics with a two-stage tube

1. Spherical mirrors.
2. Meniscus corrector.
3. Schmidt corrector.
4. Image tube (Du Mont unity mag. or RCA two-stage C 73458).

To provide an instrument useful in high energy physics, a complete image tube system should consist of a first ungated tube with a fast (one microsecond decay time) phosphor such as P15 for fast storage, and a second tube using a fast gate (one or two microseconds) followed by an image tube system with high amplification. Thus the first tube stores the image momentarily while other electronics determine from various counters whether or not to gate the second tube on; the following tube system may then use slower, more efficient phosphors to provide maximum gain. The time resolution of luminescent chamber is then determined by the decay time of the first phosphor and the gate length applied to the second tube. The dead time is determined by the phosphor decay times on the later tubes.

With either a filamentary chamber or homogeneous chamber it is desirable to use the large cathode diameter Westinghouse tube as the first, fast phosphor tube; the following tubes in systems in general use consist of the RCA two-stage tubes.

A cascaded image tube system being used by the authors at the Berkeley Bevatron is illustrated in Fig. 6. The tubes themselves are largely concealed by their magnetic shields.

Several other image tube systems are being developed. Magnetically focused one and two-stage tubes should make possible improved resolution. An alternative approach to magnetically focused multi-stage tubes, making use of transmission secondary electron emission in thin foils, is being pursued [5]. A system employing fine metallic mesh structures, stacked in registry and insulated from each other as a channeled electron multiplier is being developed by

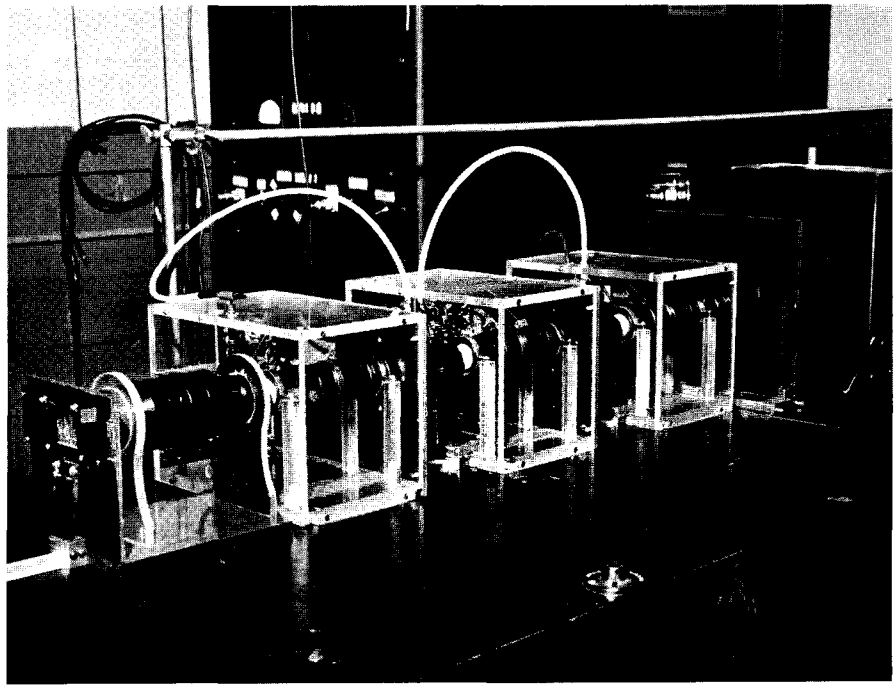

Fig. 4 Photograph of cascade geometry. Film may be located on the bakelite board to the left. The light phosphors of the three image tubes, type RCA C 73458 are visible next to the coupling lenses. The scintillator is at the right but is not visible in this photograph.

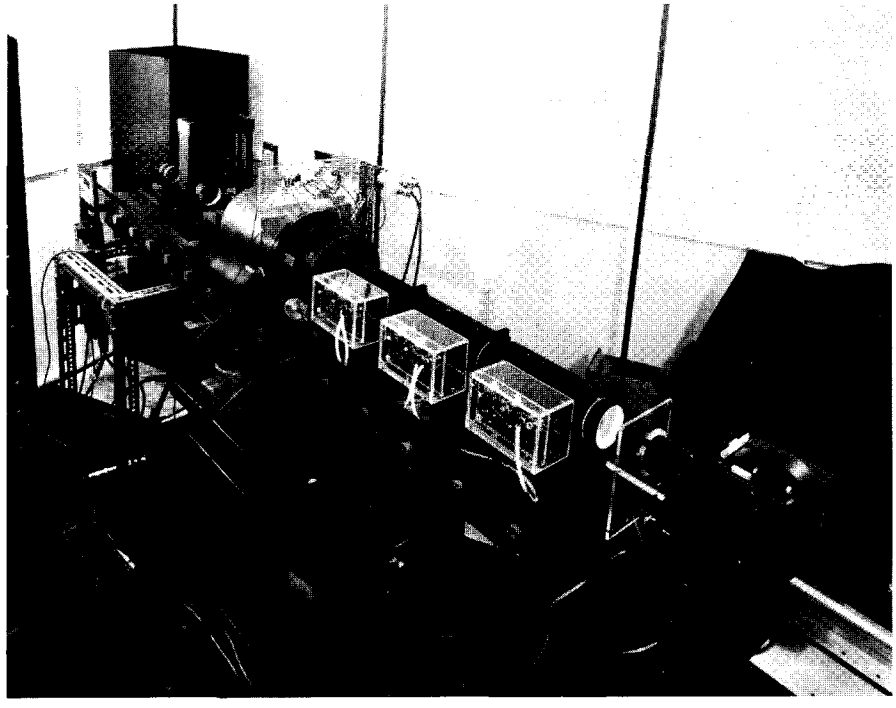

Fig. 6 Geometry in use for tests at the Berkeley Bevatron. A small scintillator is visible at the top of the optical bench behind a lens. The large tube and the three small two-stage tubes are concealed by their magnetic shields. The camera and camera lens are at the bottom right.

the Chicago Midway Laboratories. This shows promise of providing a very compact, physically strong image tube structure. Results will be given in a later paper on a three-stage electrostatically-focused tube.

Until recently, most photosensitive devices employed cesium-antimony cathode surfaces which characteristically had an efficiency of 7% to 10% for conversion of photons near 4400 Å to photo-electrons. Photomultipliers and image tubes are now available with multi-alkali cathodes which have measured efficiencies as high as 30%.

Together with the improving technology of glass fiber optics and the increasing availability of good lens optics, these various image tube developments show promise of providing continuing improvement in gain, resolution, background noise, freedom from distortion, and reliability.

IV. PARTICLE TRACK PHOTOGRAPHY

A. Homogeneous chamber

The first particle tracks were recorded from particles passing through homogeneous crystals of alkali halide scintillators. The relevant geometry is presented in Figure 7. A lens will subtend a fraction ω of the 4π solid angle of light given by

$$\Omega = \frac{a^2}{d^2}$$

where a is the radius subtended by the cone of light subtended by the lens, on the crystal surface and d is the crystal thickness. If the focal plane of the lens is at the center of the crystal, a is the maximum uncertainty in the point of origin of a photon near the edge of the crystal. If the crystal produces N photons per cm of minimum-ionizing track and the first image tube cathode efficiency is e, the number of recorded photo-electrons per cm of track in the crystal is given by n, where

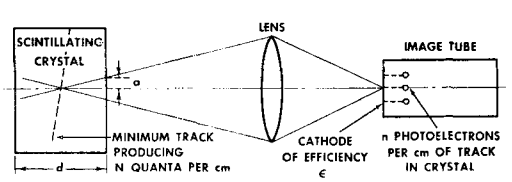

Fig. 7 Homogeneous chamber geometry.

$$n = N\Omega e = N\frac{a^2}{d^2}e\,.$$

A compromise is necessary between resolution, depth-of-field, and information from the track. It is reasonable to consider using lens apertures such that

$$n \simeq \frac{1}{a}\,.$$

In this case, $a = d^{2/3}/(Ne)^{1/3}$.

Table II gives values of a and d for thallium-activated sodium iodide and cooled cesium iodide for a 20% efficient photocathode. The transverse dimensions of the crystal may be very large; if the image tube system has a resolution of M lines across the diameter of the useful field, a reasonable scintillator diameter would be Ma. This is subject to the constraint that the lens focusing the crystal onto the first cathode must not operate at an Ω and a demagnification such that it subtends an aperture from the image tube less than f/0.6 or so (the largest aperture of readily available lenses). Thus it is not reasonable to focus a 30 cm diameter scintillator on to a one cm diameter cathode with $a/d = 1/10$. For this reason the large cathode diameter image tubes are useful even with the homogeneous chamber. Currently, the volume of scintillator which can be viewed with good resolution is more severely limited by the image tube resolution than by the depth-of-field limitation.

TABLE II

Numerical examples of homogeneous scintillators

	NaI : Tl		CsI (77°K)
N	10^5		10^6
e		0.2	
d	10 cm		20 cm
a	1.7 mm		1.3 mm

Photographs of cosmic ray mesons passing through a 7.5 cm diameter, 6 cm thick, NaI:Tl crystal are reproduced in Figures 8 through 11. These were taken at Michigan using the image tube system of Figure 4 as described above, either alone or preceeded by a single-stage 12.5 cm cathode tube. In these photographs none of the tubes used fast phosphors and the fastest gate pulse was 500 μs. On many of the photographs the spurious dots due to image

tube noise appear. Since the background dots are initiated by many electrons, even the second and third cathodes in the system may contribute noise dots as bright as single photo-electrons from the first cathode.

It should be noted that rather large volumes even of plastic scintillator may be used if a is relaxed to of the order of one centimeter. In this way the general outline of a very high energy event may be observed. At the other extreme, Zavojskij [6] has photographed α particle tracks in scintillators 25 microns long with one micron resolution using a 250 × microscope.

Larger scintillator volumes than listed in Table II may be used with good resolution by using more than one image tube-camera system, each focused at a different depth in the scintillator or at a different area.

B. Filamentary chamber

Filaments or fibers of plastic scintillator may be used to circumvent the depth-of-field resolution paradox as suggested by Kerth and by Reynolds [7]. In this system, scintillation light in each filament is " piped " to the end by total internal reflection. Thus the spatial resolution of a track is determined by the diameter of filaments in a scintillator filament matrix and is independent of their length. Filament chambers and their couplings to image tubes are represented schematically in Figures 12 and 13. Stereoscopic presentation of an image is obtained by orienting alternative layers of filaments at right angles and viewing two faces of the cube with two image tube systems. The average number of photo-electrons produced from the first image tube per cm of minimum-ionizing track is given by

$$n = Ne\Omega P$$

where Ω is the fraction of the 4π solid angle subtended

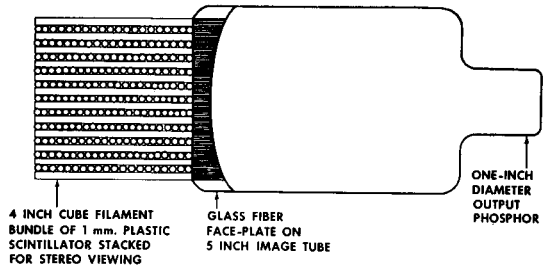

Fig. 12 Filamentary chamber using glass light-pipe tube envelope (schematic).

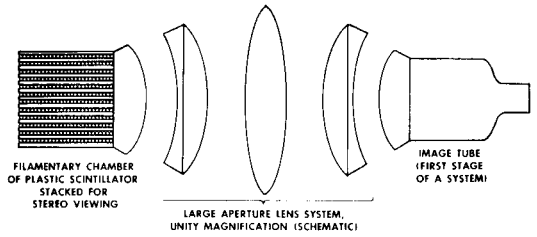

Fig. 13 Filamentary chamber using large aperture optical coupling to first image tube (schematic).

by light totally internally reflected and P is the scintillator packing factor [3]. For Ω of 15%, N for plastic scintillator of 10^4, e of 20%, and P of 1/3, n is 100. Since half the filaments lie at right angles, P will be less than 1/2; if the filaments are cylindrical rather than square in cross-section it will be further reduced. If the filaments are 1/2 mm diameter, one may expect approximately five photo-electrons per filament. If the filaments are demagnified to a diameter comparable to the image tube resolution, the required image tube gain may be less than that required for recording of single photo-electrons; if larger filament diameters are used, or if losses occur in the optical coupling, a gain sufficient to record single photo-electrons is again required.

As indicated in Figures 12 and 13, a major problem in using a filamentary chamber is the coupling of light from the filaments to the first image tube. Since the angle for total internal reflection is large, the optics must have a correspondingly large aperture to be useful. It follows from general principles of optics, therefore, that the image tube cathode must have a cathode diameter comparable to the chamber cross-section independent of whether refractive optics, reflective optics, or glass fiber optics are used. Thus, the depth-of-field problem of the homogeneous chamber is exchanged for a diameter-of-field problem in the filamentary chamber, although again multiplying the number of image tube systems relaxes the constraint. It should be noted that the 12.5 cm cathode Westinghouse image tube will be available with a glass fiber cathode envelope, and alternatively a lens system of unity magnification and 12.5 cm diameter field has been designed with an aperture of f/1.5. A practical problem has been the production of scintillator filaments free from surface defects limiting total internal reflection Thus currently available filaments have an attenuation mean free

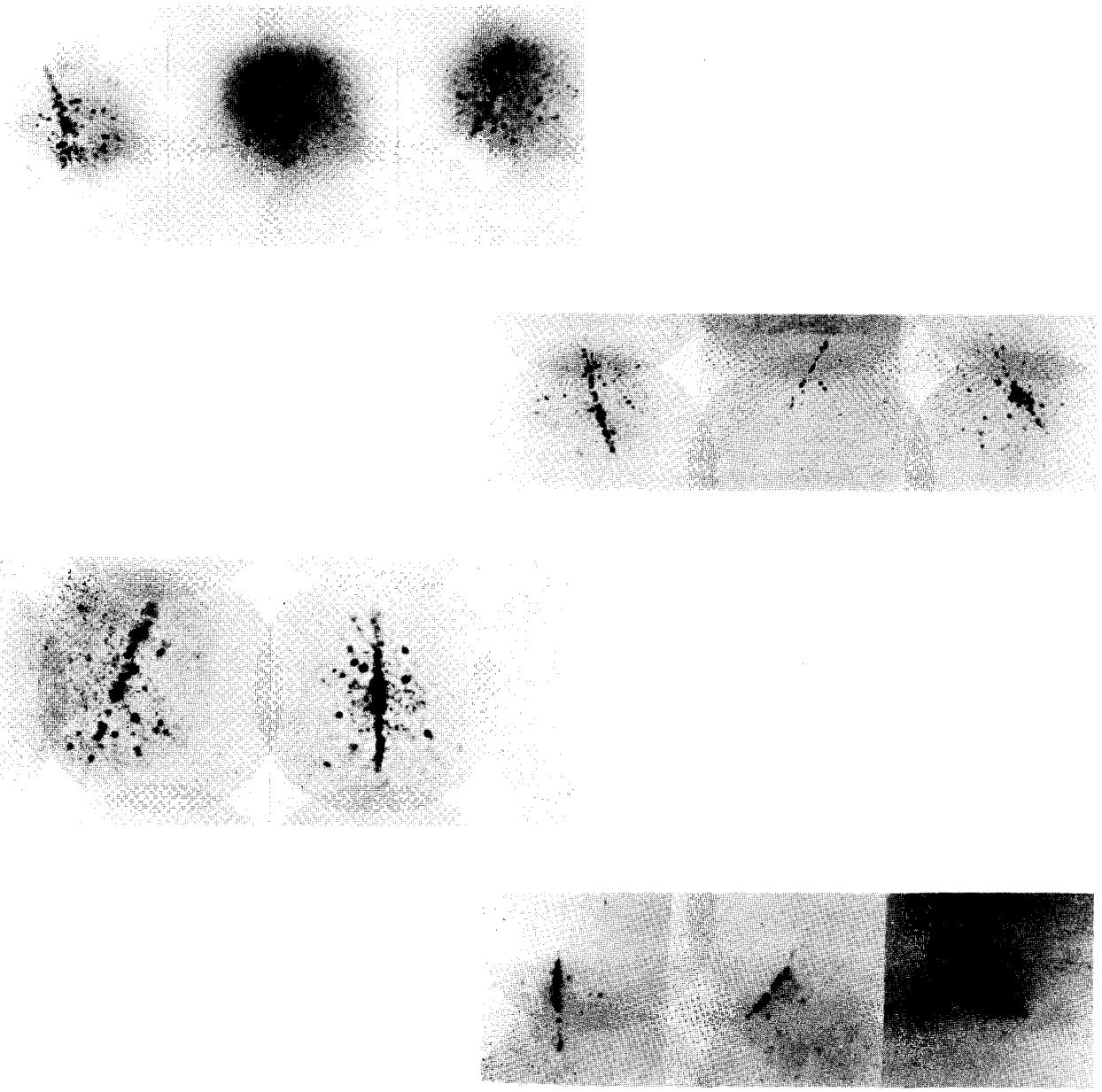

Figs. 8-11 Photographs of cosmic ray tracks in a 7.5 cm diameter 6 cm thick NaI: Tl crystal using three and four image tubes in cascade.

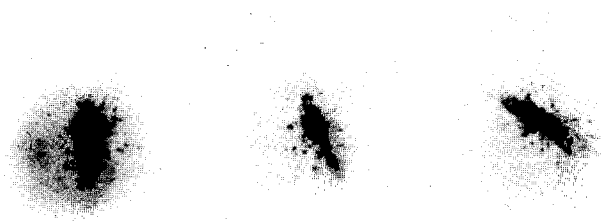

Fig. 14 Photographs of cosmic ray tracks in scintillator filaments butted against the five inch cathode envelope.

path of from 10 to 30 cm for the totally internally-reflected light. This technical problem should yield to solution as improved fabrication procedures are evolved.

Photographs have been taken of plastic scintillator filaments using bundles of filaments simply butted against the cathode envelope of the image tube. Figure 14 illustrates tracks taken in this manner with the authors' system. In addition, the groups at the University of Pensylvania, Princeton University, and at Massachusetts Institute of Technology have obtained track photographs with filaments.

Filaments of inorganic scintillator have been considered and will be useful should they become available. It should be noted that the ultimate resolution of filaments is given simply by the optical cut-off diameters of filaments considered as wave-guides. Such effects have been observed with glass fibers of diameters of the order of microns. The number of recorded photo-electrons per cm of track should approach the value of 100 given above, so that in the limit, filamentary chambers could provide excellent resolution and track information.

V. UTILITY OF THE LUMINESCENT CHAMBER

As a result of work within the past year, four groups in the U.S. have photographed tracks of cosmic rays in filamentary or homogeneous luminescent chambers. Together with Zavojskij's earlier work, there is thus ample evidence of the fundamental practicality of the luminescent chamber. The coming year should see the use of both types of luminescent chambers, with dimensions of the order of 10 to 20 cm, in high energy physics.

TABLE III

Comparison of detection devices

Device	Space resolution	Time resolution	Dead time
Emulsion	10^{-4} cm	10^{4} s	
Bubble chamber	10^{-2} cm	10^{-3} s	>1 s
Luminescent chamber	10^{-1} cm	$>10^{-6}$ s	10^{-3} s
Counter arrays	>1 cm	10^{-9} s	10^{-7} s

To place the chamber in its proper perspective, Table III summarizes some relevant properties of various detectors. The luminescent chamber is seen to display a space and time resolution intermediate between bubble chambers and counters. While a luminescent chamber cannot use pure hydrogen for the sensitive volume, it can be instructed to record only events of interest (analogous to the post-expansion cloud chamber). Ultimately the time resolution of the luminescent chamber is limited only by the transit time of light and particles across the chamber; 10^{-8} s for a chamber with dimensions of the order of one meter. In practice, the time required for the gating information from the counters to turn on the second image tube is 0.1 to 0.2 μs, due to photomultiplier transit times, pulse delays through fast amplifiers, and turn-on time of gate pulses of several kilovolts. This makes it difficult to use phosphors faster than P15, and therefore currently limits the resolving time to the order of one microsecond. In comparison with the bubble chamber, it should be noted that 90° stereoscopic viewing will be the general rule with the luminescent chamber.

The greatest use of the luminescent chamber appears to lie in the recording and study of rare interactions too complex to analyze readily by counter arrays. Thus at 10 tracks per picture, the large hydrogen bubble chambers can accumulate at most about 10^{7} events per year. If a particular interaction has a frequency of 10^{-5}, the bubble chamber could collect and study only 100 per year of this type. However if this interaction can be made to leave a characteristic counter signature, this counter pulse can trigger a luminescent chamber to record only those events such that each photograph will contain only the event of interest. On the other hand, if the event involves three or more outgoing particles whose subsequent interaction is of interest, it is difficult to analyze by counters alone. A few typical proposed luminescent chamber experiments of interest currently in physics are enumerated below.

Σ^{+} scattering

Using the reaction

$$\pi^{+}+P\rightarrow\Sigma^{+}+K^{+}$$

a small ($5\times5\times10$ cm) scintillation chamber may be placed in a π^{+} beam and instructed to photograph only events where a π^{+} enters and a K^{+} leaves the volume (as determined by a π Cherenkov counter

and a K^+ detector of the type developed by Cool and Cronin [8]). In NaI, approximately 10% of the Σ^+ may be expected to scatter before decaying, and a nuclear scattering cross-section should be obtainable. A homogeneous plastic scintillator $5\times5\times12$ cm may then be substituted with a resolution of about a millimeter (since the particles of greatest interest, Σ^+ and P, are about twice minimum ionization) and Σ^+-P elastic scatters observed. The small scintillator volume is appropriate here because of the short decay mean free path of the Σ^+ and the high π^+ fluxes available (e.g. about 10^6 per Bevatron pulse in a momentum analyzed beam).

$K^+ + P$ inelastic scattering

The reaction $K^+ + P \rightarrow K + P + \pi$ can furnish information concerning the $K-\pi$ interaction [9]. A liquid hydrogen target along the axis of a sodium iodide scintillator may be used as indicated schematically in Figure 15. K mesons entering but not leaving the target would trigger a photograph, and a fraction of the $K-P$ interactions should show up as inelastic events. π° mesons would be detected with moderate efficiency in a chamber of these dimensions ($10\times10\times25$ cm). A single image tube system could be used to record both stereo views by using mirrors to direct both rectangular images side by side on to the same cathode. Similar experiments could be done on $\pi+P\rightarrow\pi+\pi+P$. K meson fluxes of the order of 10^3 per Bevatron pulse are available in momentum-analyzed, mixed beams.

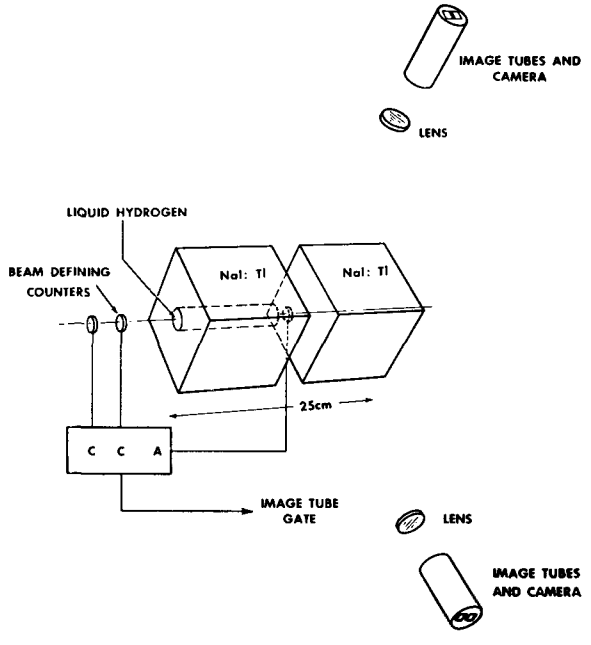

Fig. 15 Stereoscopic luminescent chamber geometry for study of reactions such as $K^+ + P$. Image tube systems indicated very schematically.

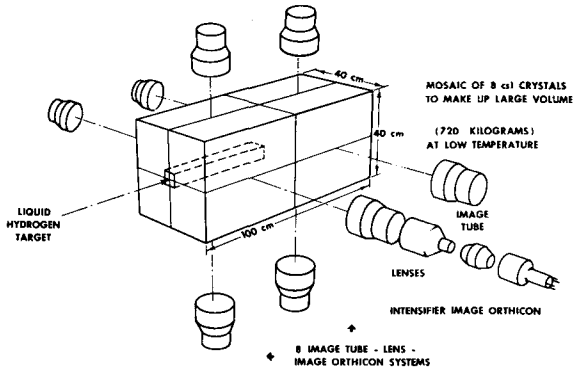

Fig. 16 Projected large homogeneous scintillation chamber.

Λ magnetic moment

A separate paper at this Symposium discusses this experiment as planned by the MIT group. It will only be noted here as typical of the cases where counter triggering of the chamber makes the experiment practical in a finite time. Both this and the $\pi+P\rightarrow\pi+\pi+N$ experiment are also planned by counter groups, however they can be done more simply and cleanly with a good luminescent chamber.

$K^- + P \rightarrow K^+ + \Xi^-$

Counter detection of K^- in and K^+ out of a hydrogen target would define Ξ^- particles entering a luminescent chamber of the type of Fig. 15 allowing systematic study of Ξ^- particles. Unfortunately the K^- fluxes from the Bevatron are a little low for this experiment to collect more than a few Ξ^- per hour. The MIT group has proposed using a filamentary chamber to study all K^- interactions in plastic scintillator at 1 to 3 BeV/c K^- momentum.

VI. THE FUTURE OF THE LUMINESCENT CHAMBER

The efficient utilization of very high intensity (10 to 100 μA) multi-BeV FFAG accelerators will require detectors of good time resolution capable

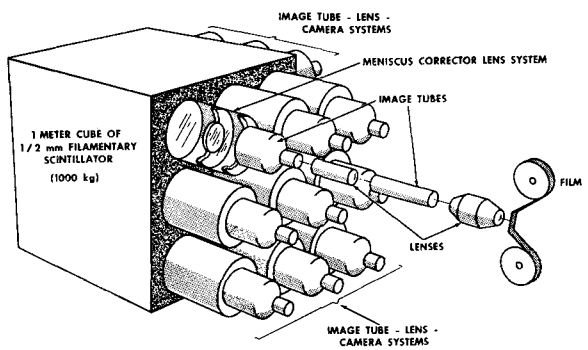

Fig. 17 Projected large filamentary chamber.

of studying the more complex events. The luminescent chamber promises to fit this need. Chambers and counters may well lose their separate identity in some types of experiments, where complex arrays of scintillators may be viewed by image tubes and photographed or recorded on magnetic tape rather than fed to individual photomultipliers. Scintillation chambers can make use of momentum-analyzed beams of mixed particles using velocity sensitive counters without requiring electrostatic separators. This should allow closer approach and larger solid angles for beams of short-lived particles such as K mesons.

The very large luminescent chambers of homogeneous or filamentary scintillator one might imagine are indicated in Figures 16 and 17. In either case spatial resolution of about a millimeter is maintained. In the homogeneous chamber, each image tube system views a $40\times40\times20$ cm volume of scintillator with each $40\times20\times20$ cm prism of crystal viewed stereoscopically at approximately 90° by two image tubes. The image tube lens systems viewing the cubic meter filamentary chamber must demagnify the image from the filaments to permit the entire volume to be viewed. For sufficiently good filaments and very good optics, a 2 : 1 demagnification should be possible while still recording an average of more than one photo-electron per filament through which a particle passes.

The potentialities of the luminescent chamber might be most impressively used with colliding beam devices to explore extremely high energy proton-proton interactions. A suggestion of some of the geometries which might be useful in this context is given in another paper at this Symposium.

VII. OTHER DETECTORS

The luminescent chamber is subject to fundamental improvements. If the scintillator light output were enhanced through electric or magnetic fields, RF or ultraviolet excitation, or changes in pressure or temperature, better luminescent chambers could be realized. These subjects remain largely unexplored. New scintillators may be found; in particular, it would be very useful to find some material with which to dope liquid hydrogen to cause it to scintillate.

Other detectors may also be developed. A possible gas scintillation chamber is indicated in Figure 18. Here a gas such as argon in a uniform magnetic field has an electrical field pulse perhaps one microsecond long applied to it following an event of interest. Electron multiplication should occur along the lines of magnetic field, and a scintillation pattern corresponding to a two dimensional projection of the event should appear on a screen normal to the magnetic field for applied electric fields of the order of 10 kV per cm. Decays at low velocity of strongly interacting particles such as K^- mesons might be studied in this way.

Solid state devices such as the new silicon α particle counters might be arranged in a solid matrix with counting information read off faces of the matrix by a scanning electron beam.

Fukui and Miyamoto [10] have succeeded in making a multiplate spark chamber and this may find application in some experiments.

In conclusion, it should be noted that no one detector is suitable for all the important experiments in high energy physics, and the luminescent chamber is no exception. On the other hand, as physics progresses,

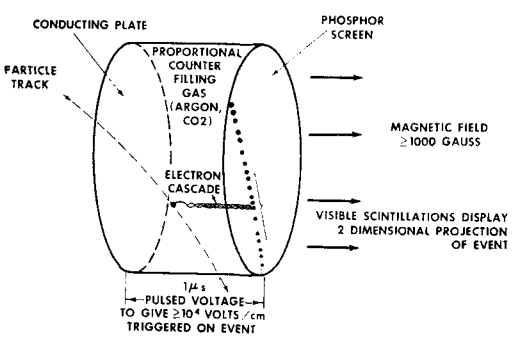

Fig. 18 Possible gas scintillation chamber.

it should be expected that new situations will continue to arise requiring unanticipated characteristics of detectors and novel techniques. The luminescent chamber appears to add a potentially powerful tool to the arsenal of techniques available to the experimental physicist, and it is entirely reasonable to expect other detectors of unique properties to continue to be conceived, developed, and used.

LIST OF REFERENCES

1a. Zavojskij, E. K., Smolkin, G. E., Plakhov, A. G. and Butslov, M. M. Lyuminestsentniya kamera. (Luminescence camera). Doklady Akad. Nauk. SSSR, *100*, p. 241-2, 1955.

b. Zavojskij, E. K., Butslov, M. M., Plakhov, A. G. and Smolkin, G. E. O lyuminestsentnoj kamere. Atomnaya Energiya, *1*, p. 34-7, 1956 (in Russian); A luminescence camera. J. Nuclear Energy, *4*, p. 340-4, 1957. (in English).

c. Perl, M. L. and Jones, L. W. Photography of cosmic rays in a luminescence chamber. Phys. Rev. Letters, *2*, p. 116-7, 1959.

d. Jones, L. W. and Perl, M. L. Luminescent chamber technical report No. 1. University of Michigan, 1958 (unpublished).

e. Lande, K., Mann, A. K., Schlachter, M. M., Skyrme, D. M. and Uto, H. Photographic observation of charged particles in a filamentary chamber. Rev. sci. Instrum., *30*, p. 496-7, 1959.

f. Reynolds, G. T., Giacconi, R. and Scarl, D. Cosmic ray tracks in filament scintillation chambers. Rev. sci. Instrum., *30*, p. 497-8, 1959.

2a. Hahn, B. and Rossel, J. Scintillations des particules α dans CsI. Helv. Phys. Acta, *26*, p. 271-80, 1953.

b. Hahn, B. and Rossel, J. Scintillations dans CsI et spectrométrie γ. Helv. Phys. Acta, *26*, p. 803-10, 1953.

c. Hahn, B. Scintillations produced by alpha particles in CsI. Phys. Rev., *91*, p. 772-3, 1953.

d. Knœpfel, H., Lœpfe, E. and Stoll, P. Untersuchungen an anorganischen Szintillations-Phospheren unter besonderer Berücksichtigung von Cäsiumjodid. Helv. Phys. Acta, *30*, p. 521-52, 1957.

3. Kapany, N. S. Fiber optics. Pt. I J. opt. Soc. Amer., *47*, p. 413-22, 1957.

4a. Jones, L. W. and Perl, M. L. Experimental demonstration of electron-optical regenerative image amplification. Rev. sci. Instrum., *29*, p. 441-2, 1958.

b. Jones, L. W. Current status of the luminescent chamber. MURA (*) 416, July *31*, 1958.

c. Perl, M. L. and Jones, L. W. In : Symposium on scientific uses of photo-electronic image devices. Proceedings. London, Imperial College. (to be published).

d. Jones, L. W. and Perl, M. L. In : U.S.A.E.R.D.L. Image Tube Symposium. Proceedings (to be published).

5. Sternglass, E. J. and Wachtel, M. M. Transmission secondary electron multiplication for high resolution counting and imaging. Phys. Rev., *100*, p. 1238, 1955.

6. Zavojskij, E. K. and Smolkin, G. E. O mezhmolekulyarnom perenose energii vozbuzhdeniya v kristallakh. Doklady Akad. Nauk SSSR, *111*, p. 328-30, 1956 (in Russian); On the intermolecular transfer of excitation energy in crystals. Soviet Physics, Doklady, *1*, p. 652-4, 1956. (in English).

7. Reynolds, G. T. and Condon, P. E. Filament scintillation counter. Rev. sci. Instrum., *28*, p. 1098-9, 1957.

8. Cool, R. L., Cork, B., Cronin, J. W. and Wenzel, W. A. A symmetry in the decay of Σ hyperons. UCRL (*) 8539, November 1958.

9. Chew, G. F. and Low, F. E. Unstable particles as targets in scattering experiments. Phys. Rev., *113*, p. 1640-8, 1959.

10. Fukui, S. and Miyamoto, S. A new type of particle detector : the " discharge chamber ". Nuov. Cim., *11*, p. 113-5, 1959.

(*) See note on reports, p. 696.